The Finite Element Method with FreeFem++ for beginners

Article *in* The Electronic Journal of Mathematics and Technology · June 2013

2 authors:

Roberto Font
Biometric Vox
17 PUBLICATIONS 57 CITATIONS
SEE PROFILE

Francisco Periago
Universidad Politécnica de Cartagena
50 PUBLICATIONS 306 CITATIONS
SEE PROFILE

The Finite Element Method with FreeFem++ for beginners

Roberto Font and Francisco Periago
e-mail: roberto.font@upct.es - f.periago@upct.es
Department of Applied Mathematics and Statistics
Universidad Politécnica de Cartagena
30202 Cartagena
Spain

Abstract

These notes are concerned with the numerical resolution of Partial Differential Equations (PDE) by the Finite Element Method (FEM). Emphasis is placed in the practical numerical resolution of this type of problems by using the free software FreeFem++. Theoretical background is briefly reviewed (without entering in technical details) and a number of examples are given, along with the code. The goal is to introduce in a simple way this difficult (but very interesting in real-world applications) topic to undergraduate students who do not have a solid background both in variational methods and in numerical analysis for PDE.

1 Introduction

Mathematical modeling is the art of representing a physical phenomenon in mathematical terms. Most of these models (equations of linear elasticity, Navier-Stokes equations of fluid mechanics, Maxwell equations of electromagnetism, etc...) are written as a partial differential equation (PDE) or a system of PDE defined on a suitable domain of $\mathbb{R}^n$, $n = 1, 2, 3$. Boundary (and possibly initial) conditions complete the model. The interest in Industry of solving numerically these problems is nowadays unquestionable. Therefore, these aspects of Mathematics should be considered as an essential part of education in schools of mathematics, physics and engineering.

In these notes, we focus on the numerical resolution of PDE problems by the Finite Element Method (FEM). Our goal is twofold: (i) first, we aim at introducing FEM to undergraduate students who have received some very preliminary courses on linear algebra and calculus, and (ii) we shall illustrate the power of this method by solving a number of specific examples with the free software FreeFem++. Of course, there is a number of wonderful books (e.g., [6]) dealing with the numerical resolution of PDE and there is also a tutorial for FreeFem++ [3]. These notes do not aim at replacing or completing those references. We just will try to collect the main aspects of this topic in a simple way in order to make it accessible to students without a solid background on the theoretical ingredients underlying to FEM.

The rest of the paper is organized as follows. In Section 2 we briefly review on the FEM. Then, in Section 3 we follow the Learning by Examples method to illustrate how to use FreeFem++ to solve a number of interesting PDE problems by the FEM.

2 A review on the Finite Element Method

Next, we shall describe the FEM through a very simple one-dimensional model. Part of the material of this section has been adapted from [4, 5].

2.1 A very simple one-dimensional model in linear elasticity

Consider a perfectly elastic and flexible string stretched along the segment $[0, L]$. Assume that on the string acts a vertical force $f = f(x)$ and that the string is fixed at both endpoints.

Hooke's law on linear elasticity and the momentum conservation law lead to the equation $-(\kappa u')' = f$ in $(0, L)$, where $\kappa = \kappa(x) \geq \kappa_0 > 0$ depends on the physical properties of the string. Thus, the mathematical model for this problem is

$$\begin{cases} -(\kappa u')' = f & \text{in} \quad (0, L) \\ u(0) = u(L) = 0. \end{cases} \tag{SP}$$

Assume now that the external force is located at $x = L/2$. It is clear that physically we would observe something like in Figure 1.

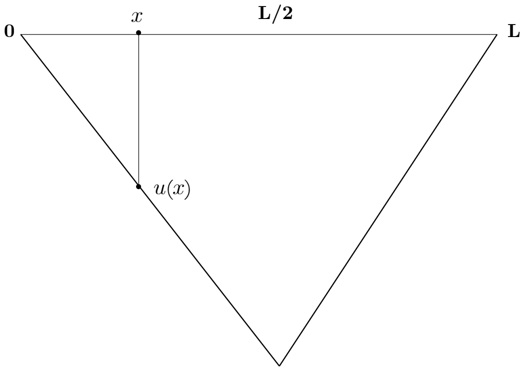

Figure 1: String fixed at its ends carrying a load at $x = L/2$.

But a function as given in the preceding picture is not differentiable at $x = L/2$. Hence, such a function cannot be a solution of a second-order differential equation $-(\kappa u')' = f$ in $(0, L)$, at least in the classical sense, that is, in the sense of being u twice differentiable at each point of the open interval $(0, L)$ and satisfying the differential equation point-wise in that interval. This simple example shows that it is necessary to look for a new concept of a solution of a differential equation.

2.2 Variational formulation of a differential equation

Instead of looking at the conservation of momentum principle, we may start from the virtual work principle. This way, if the force f produces a virtual displacement $v(x)$ at a point x, then the work produced by $f(x)$ is $f(x)\,v(x)$ so that the work produced by f along the whole string is given by

$$\int_0^L f(x)\,v(x)\;dx.$$

Proceeding in the same way in the left-hand side of the equation in problem (SP) and integrating by parts,

$$\int_0^L -\left(\kappa(x)\,u'(x)\right)'v(x)\;dx=\int_0^L \kappa(x)\,u'(x)\,v'(x)\;dx,$$

since $v(0)=v(L)=0$. This process transforms the differential equation $-(ku')'=f$ into the integral equation

$$\int_0^L \kappa(x)\,u'(x)\,v'(x)\;dx=\int_0^L f(x)\,v(x)\;dx, \tag{1}$$

which as indicated above reflects virtual work principle in Physics. Hence, we may think in a solution of problem (SP) as a function $u:[0,L]\to\mathbb{R}$, with $u(0)=u(L)=0$, which satisfies (1) for all possible displacements v such that $v(0)=v(L)=0$. One of the main advantages of this approach is that we have reduced the requirements that the function u ought to satisfy. Nevertheless, there are still two main points which are not clear for the present moment:

(1) u should be at least once differentiable, but this is not the case for a charge located at a point.

(2) if the charge is located at $x=L/2$ (that is, $f(x)=0$ for all $0\le x\le L$, $x\ne L/2$), then $\int_0^L f(x)\,v(x)\,dx=0$ so that $u=0$ satisfies (1), in contradiction with physical experience (see Figure 1).

The above shows that it is necessary to understand better the way of dealing mathematically with the concept of a charge located at a point. As a first approach, let us consider that the charge is distributed in a small portion around $x=L/2$, that is,

$$f_\varepsilon(x)=\begin{cases}1/(2\varepsilon), & \frac{L}{2}-\varepsilon\le x\le\frac{L}{2}+\varepsilon\\ 0, & \text{otherwise}\end{cases}$$

The work produced by this charge with a displacement v is now given by

$$\int_0^L f_\varepsilon(x)\,v(x)\;dx=\int_{\frac{L}{2}-\varepsilon}^{\frac{L}{2}+\varepsilon}\frac{v(x)}{2\varepsilon}\,dx=v(\xi_\varepsilon),$$

where $\frac{L}{2}-\varepsilon\le\xi_\varepsilon\le\frac{L}{2}+\varepsilon$, and the equality being a consequence of the mean value theorem for integrals. Now letting $\varepsilon\to0$ and assuming v is continuous it is concluded that, in this sense, the work produced by a single charge located at $L/2$ and producing a displacement $v=v(x)$ is $v(L/2)$. This reasoning shows that we can deal mathematically with a single charge located at a point x_0 as a mapping, say δ_{x_0}, which acts on a certain class of functions and produce numbers by following the rule

$$\delta_{x_0} : v \mapsto < \delta_{x_0}, v >=^{\text{def}} v\left(x_0\right).$$

All of this makes a rigorous sense in the framework of the theory of distributions developed by the French mathematician L. Schwartz in 1946, and this is basically the mathematical background we need to formulate precisely our boundary value problem. Next we briefly review some of the main aspects of this theory.

Given an open interval $I \subseteq \mathbb{R}$, $\mathcal{D}\left(I\right)$ stands for the *test functions space* composed of all functions $v : I \to \mathbb{R}$ which are indefinitely differentiable and have compact support[1] in I. Now given a sequence $\{v_n\}_{n=1}^{\infty} \subseteq \mathcal{D}\left(I\right)$ it is said that this sequence converges to $v \in \mathcal{D}\left(I\right)$ if (i) there exists a compact set $K \subseteq I$ such that supp $v_n \subseteq K$ for all $n \in \mathbb{N}$, and (ii) for each $m \in \mathbb{N}$, $\frac{d^m}{dx^m} v_n$ converges uniformly to $\frac{d^m}{dx^m} v$.

A distribution u is defined as a linear and continuous (with respect to the above notion of convergence) mapping $u : \mathcal{D}\left(I\right) \to \mathbb{R}$. Let us now show the two typical examples of distributions.

- If $f : I \to \mathbb{R}$ is locally integrable, then a distribution u_f may be associated with f by means of the mapping

  $$u_f : \mathcal{D}\left(I\right) \to \mathbb{R}, \quad v \mapsto < u_f, v >=^{\text{def}} \int_I f\left(x\right) v\left(x\right)\, dx.$$

  It is very common to denote by f the distribution u_f. In what follows we use this notation.

- Given $x_0 \in I$, it is not hard to show that the mapping

  $$\delta_{x_0} : \mathcal{D}\left(I\right) \to \mathbb{R}, \quad v \mapsto < \delta_{x_0}, v >=^{\text{def}} v\left(x_0\right)$$

  is a distribution. This distribution is called the Dirac delta (or Dirac mass).

Next, we wish to do calculus with distributions. In particular, we wonder if it is possible to define the derivative of a distribution. Assume first that $f : I \to \mathbb{R}$ is a differentiable function and take $v \in \mathcal{D}\left(I\right)$. From the distributions point of view, the derivative of f is given by $\int f'v$, but integrating by parts and taking into account that v vanishes at the extremes of I it is concluded that $\int f'v = -\int fv'$, that is, in the language of distributions

$$< f', v >= - < f, v' > .$$

In general, given a distribution u, its distributional derivative is defined as the distribution u' given by

$$< u', v >= - < u, v' > \quad \text{for all } v \in \mathcal{D}\left(I\right). \tag{2}$$

Notice that, contrary to what happens with functions, a distribution may be derived infinitely times.

Once we have at one's disposal distributions, let us go back to (SP) or in particular to the integral equation (1). Let $L^2\left(0, L\right)$ denote the Hilbert space of functions $f : \left(0, L\right) \to \mathbb{R}$ of square integrable endowed with the norm $\|f\|_2 = \left(\int_0^L f^2\left(x\right) dx\right)^{1/2}$. In order to the right-hand side of (1) to make

[1] the support of a continuous function v is defined as supp $v = \overline{\{x \in I : v\left(x\right) \neq 0\}}$.

sense, by the Cauchy-Schwarz inequality, all we need is to have $f, v \in L^2$. As for the left-hand side of (1), if we assume κ to be bounded, then we just need $u', v' \in L^2$. As usual, we denote by

$$H_0^1(0,L) = \left\{u \in L^2(0,L) : u' \in L^2(0,L),\ u(0) = u(L) = 0\right\},$$

which endowed with the norm $\|u\|_{H_0^1} = \left(\|u\|_2^2 + \|u'\|_2^2\right)^{1/2}$ is a Hilbert space. Of course, the derivatives in this space are understood in the sense of distributions. It can be proved that the test functions space $\mathcal{D}(0,L)$ is $\|\cdot\|_{H_0^1}-$dense in $H_0^1(0,L)$. From this it follows that the Dirac delta can be extended to a linear and continuous form $\delta_{x_0} : H_0^1(0,L) \to \mathbb{R}$, acting as $< \delta_{x_0}, u >= u(x_0)$, with $u \in H_0^1$. Functions f of L^2 may be also considered as linear and continuous forms on H_0^1 just by defining it as

$$f : H_0^1 \to \mathbb{R}, \quad v \mapsto < f, v > =^{\text{def}} \int fv.$$

These new ideas lead to a new formulation of (SP). Precisely, given a linear and continuous form $f : H_0^1 \to \mathbb{R}$ and the bilinear form

$$a : H_0^1 \times H_0^1 \to \mathbb{R}, \quad (u,v) \mapsto a(u,v) = \int_0^L \kappa(x)\, u'(x)\, v'(x)\ dx$$

a function $u \in H_0^1$ is said to be a *weak solution* of (SP) if the identity

$$a(u,v) = < f, v >$$

holds for all $v \in H_0^1$. The existence and uniqueness of a weak solution is usually obtained through a Lax-Milgram type theorem [2, p. 297].

2.3 The Finite Element Method

We are now in a position to describe the FEM. We already know that the solution of our problem lives in a Hilbert space like H_0^1. The main difficulty is that this space is too big. Precisely, it is infinite-dimensional. The basic idea of the FEM consists of approximating the big space H_0^1 by some appropriate finite-dimensional spaces H_h, where h is a positive parameter, satisfying the following conditions:

(a) $H_h \subseteq H_0^1$,

(b) in H_h we can easily solve the variational problem and hence obtain a solution u_h, and

(c) when $h \searrow 0$, $H_h \nearrow H_0^1$.

This procedure leads to a numerical approximation u_h of the weak solution u of our original problem. Let us show how this method works for the case of the (SP) problem.

Construction of H_h

Let $n \in \mathbb{N}$ and $h = 1/(n+1)$. The interval $[0,L]$ can be decomposed as

$$[0,L] = \bigcup_{i=0}^{n} [c_i, c_{i+1}], \quad c_i = ih,\ 0 \le i \le n.$$

Now set

$$H_h = \left\{ v : [0, L] \to \mathbb{R} \text{ continuous, } v(0) = v(L) = 0 \text{ and } v|_{[c_i, c_{i+1}]} \in \mathcal{P}_1 \right\}$$

where $\mathcal{P}_1$ stands for the space of polynomials of degree less than or equal to 1. It is not hard to show that $H_h \subseteq H_0^1$. As for the dimension of H_h, the family of functions

$$\phi_i(x) = \begin{cases} 1 - \frac{|x - c_i|}{h}, & c_{i-1} \le x \le c_{i+1} \\ 0, & \text{otherwise} \end{cases}$$

for $1 \le i \le n$, is a basis of H_h. Therefore, $dim\,(H_h) = n$.

The construction of the space H_h is not unique. Other options are possible as well. Anyway, we are considering here the simplest case.

The variational problem in H_h

Since $H_h \subseteq H_0^1$ is finite-dimensional, $\left(H_h, \|\cdot\|_{H_0^1}\right)$ is a Hilbert space. Thus, the variational problem (SP) in H_h is formulated as follows: find $u_h = \sum_{i=1}^n u_h^i \phi_i \in H_h$ such that the identity

$$a(u_h, v_h) =^{\text{def}} \int_0^L \kappa u_h' v_h' \, dx = \ < f, v_h > \tag{3}$$

holds for all $v_h \in H_h$. Remember that if $f \in L^2$, then $< f, v_h > = \int_0^L f v_h$; and if f is a Dirac delta at x_0, then $< f, v_h > = v_h(x_0)$.

It is evident that if (3) holds for all $v_h \in H_h$, then it is held for all ϕ_i, $1 \le i \le n$; and conversely, since H_h is a vector space, if (3) holds for all ϕ_i, $1 \le i \le n$, then it is held for all $v_h \in H_h$. Hence, the integral equation (3) transforms into the linear system

$$\sum_{i=1}^n u_h^i a(\phi_i, \phi_j) =< f, \phi_j >, \quad 1 \le j \le n,$$

and taking into account the properties of the functions ϕ_i, this system is written as

$$\left\{ \begin{array}{lcl} a(\phi_1, \phi_1) u_h^1 + a(\phi_2, \phi_1) u_h^2 + 0 & = & < f, \phi_1 > \\ \cdots\cdots\cdots\cdots\cdots & \cdots & \cdots \\ 0 + a(\phi_{i-1}, \phi_i) u_h^{i-1} + a(\phi_i, \phi_i) u_h^i + a(\phi_{i+1}, \phi_i) u_h^{i+1} + 0 & = & < f, \phi_i > \\ \cdots\cdots\cdots\cdots\cdots & \cdots & \cdots \\ 0 + a(\phi_{n-1}, \phi_n) u_h^{n-1} + a(\phi_n, \phi_n) u_h^n & = & < f, \phi_n > . \end{array} \right.$$

Note that since the matrix of this system is three-diagonal, a numerical method for linear systems such as the Cholesky method is suitable to solve it. As for the computation of the integrals in $a(\phi_i, \phi_j)$ and in $< f, \phi_i >$, this may be done by the mid-point rule. In higher dimensions a number of well-known methods may be used for the numerical computation of these integrals (see for instance [8]).

2.4 Extension to higher dimensions

In order to illustrate the FEM in higher dimensions we consider the following Poisson equation as the test model.

$$\begin{cases} -\nabla \cdot (c \nabla u) + au = f & \text{in} \quad \Omega \\ c\frac{\partial u}{\partial n} + qu = g & \text{on} \quad \partial\Omega. \end{cases} \tag{4}$$

Here, $\Omega \subset \mathbb{R}^N$ is a bounded domain with smooth boundary $\partial\Omega$ ($N = 2, 3$ in real-world applications), $x = (x_1, \cdots, x_N) \in \Omega$, $u = u(x)$ is the unknown , $\nabla u = \left(\frac{\partial u}{\partial x_1}, \cdots, \frac{\partial u}{\partial x_N}\right)$ is the gradient of u, $c = c(x)$, $a = a(x)$ and $f = f(x)$ are given functions defined in Ω, $q = q(x)$ and $g = g(x)$ are given functions defined on $\partial\Omega$, and finally $\frac{\partial u}{\partial n} = \nabla u \cdot n$ is the directional derivative of u with respect to the outward unit normal vector n to $\partial\Omega$. Also we recall that $\nabla\cdot$ (also denoted by div) denotes the divergence operator: given a vector field $F = (F_1, \cdots, F_N)$,

$$\text{div}(F) \equiv \nabla \cdot F = \frac{\partial F_1}{\partial x_1} + \cdots + \frac{\partial F_N}{\partial x_N}.$$

Finally, we also recall the definition of the Laplacian operator: given an scalar function $u = u(x)$, the Laplacian of u, denoted by Δu (also by $\nabla^2 u$) is given by

$$\nabla^2 u \equiv \Delta u = \text{div}(\nabla u) = \frac{\partial^2 u}{\partial x_1^2} + \cdots + \frac{\partial^2 u}{\partial x_N^2}.$$

To obtain a variational formulation of (4) we proceed as in the one-dimensional case. First we multiply the PDE by some function v and then integrate in Ω. We obtain

$$\int_\Omega [-\nabla \cdot (c\nabla u) + au]\, v\, dx = \int_\Omega fv\, dx.$$

Next, we apply Green theorem (integration by parts formula in higher dimensions) to get

$$\int_\Omega (c\nabla u \cdot \nabla v + auv)\ dx - \int_{\partial\Omega} (n \cdot c\nabla u)\ v\, d\Gamma = \int_\Omega fv\, dx,$$

where the second integral in this expression is a line integral ($N = 2$) or a surface integral ($N = 3$). Finally, we impose the boundary condition. Thus,

$$\int_\Omega (c\nabla u \cdot \nabla v + auv)\ dx - \int_{\partial\Omega} (-qu + g)\ v\, d\Gamma - \int_\Omega fv\, dx = 0 \quad \forall v. \tag{5}$$

As in the 1D case, both u and v belong to a suitable function space, but it is not necessary to enter in technical details in this first contact with FEM.

Also, a discretization procedure as in the 1D case applies. The generation of a good mesh and the definition of the corresponding finite element space may be, in practise, a very difficult task. For more details on this passage see [3, 5, 6]. Finally, we notice that we do not consider in this introductory paper the analysis of the order of convergence in the FEM. We refer the reader to [1], for instance.

3 Learning FreeFem++ by examples

FreeFem++ is a free software to solve PDE using the FEM in dimensions 2 and 3 (also 1D problems may be solved from 2D). It has been (and it is being) developed by the Laboratoire Jacques-Louis Lions (Université Pierre et Marie Curie, France). FreeFem++ runs on Windows, Linux and Mac OS. The download page is `http : //www.freefem.org`. A detailed description of the possibilities of FreeFem++ as well as a tutorial and a number of slides of courses may be found in this web site.

In order to make accessible this wonderful software to students (mainly of a master level, but also to undergraduate students in Physics, Mathematics or Engineering) who have not had a previous experience with the numerical resolution of PDE, next we show a number of illustrative examples. Some of the examples that follow have been taken (with a few small changes) from FreeFem++ tutorial. They run under FreeFem++-cs 12.4 32 version.

3.1 Poisson's equation on the unit disk

As a first example, let us consider the Poisson equation on the unit disk with zero Dirichlet boundary conditions. In its classical form, the problem reads as

$$\begin{cases} -\Delta u = f & \text{in} \quad \Omega = \{(x,y) \in \mathbb{R}^2 : x^2 + y^2 < 1\} \\ u = 0 & \text{on} \quad \partial\Omega, \end{cases} \tag{6}$$

where $u = u(x,y)$ is the unknown and f is the source term.

This problem is an acceptable mathematical model for a number of physical problems. For instance, (6) models the shape of a soap film which is glued to a ring in a plane. The shape is described as the graph $(x, y, u(x,y))$ of the vertical displacement $u(x,y)$ under a vertical pressure p in terms of force per unit area and an initial tension μ in terms of force per unit length. This way, $f = p/\mu$ in (6). The boundary condition $u = 0$ on $\partial\Omega$ in (6) indicates that the soap film is glued to the ring. Another possible application of (6) is in electrostatics where u is an electrostatic potential and $f = \rho/\epsilon$, with ρ the space charge density and ϵ the dielectric coefficient. Similar applications appear in fluid mechanics or stationary heat conduction.

The variational formulation of (6) reduces to find $u \in H_0^1(\Omega)$ such that

$$\int_\Omega \nabla u \cdot \nabla v \, dxdy = \int_\Omega fv \, dxdy \quad \forall v \in H_0^1(\Omega).$$

Next we include the code in FreeFem++ to solve this problem and comment on it. For comparison reasons we take $f = 1$. Hence, (6) has an exact solution which is given by $u(x,y) = \frac{1-\left(x^2+y^2\right)}{4}$. We may use this expression to analyze the evolution of the error (in the L^2-norm) with respect to the type of finite elements and/or the number of nodes of the mesh. All scripts files in FreeFem++ must be saved with extension .edp.

Figure 2 shows the picture of the solution obtained with the code below. As for the error, we obtain $\|u - u_h\|_{L^2(\Omega)} = 5.19123 \times 10^{-6}$.

```
// Poisson's equation on the 2D unit disk
border C(t=0,2*pi){x=cos(t); y=sin(t);} //boundary of the domain
mesh Th=buildmesh(C(1000)); // mesh with 100 points on the boundary
savemesh(Th,''mesh_malla1.msh''); // to save the mesh data
plot(Th,ps=''malla.eps''); // to plot and save the mesh
fespace Vh(Th,P1); // P1 Lagrange finite elements
Vh uh,vh; // uh,vh belong to Vh
func f=1;//source term
func u=0.25*(1-x^2-y^2); // exact solution
```

```
real L2error;
// solving the variational formulation of the problem
solve Poisson(uh,vh)= int2d(Th)(dx(uh)*dx(vh)+dy(uh)*dy(vh))
                     -int2d(Th)(f*vh)
                      +on(C,uh=0);
real [int] viso=[0.,0.05,0.1,0.15,0.2,0.25];
plot(uh,value=true,fill=true,ShowAxes=0,ColorScheme =1,
viso=viso,ps="fig_poisson2d.eps"); //to plot and save the solution
L2error=sqrt(int2d(Th)((u-uh)^2)); //  error in L^2-norm
cout<<''L2error = ''<<L2error<<endl; // to show the error
```

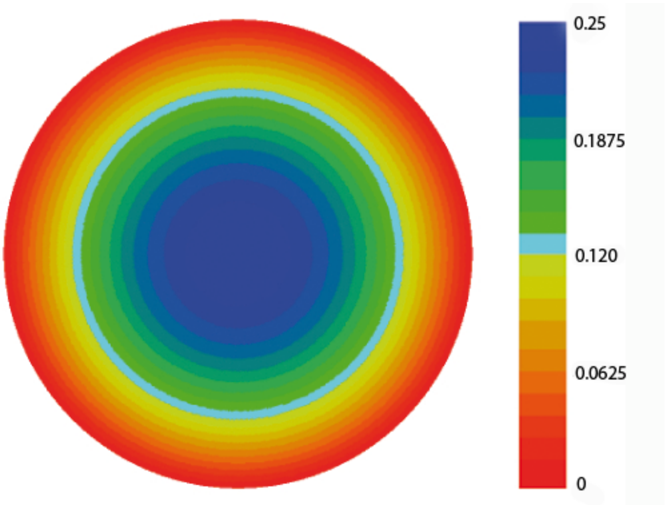

Figure 2: Picture of the solution of problem (6) obtained with the above code.

3.2 Poisson's equation on the 3D unit cube

In this example, we also consider the Poisson equation but in 3D and with a Robin-type boundary condition. There are different ways of building a 3D mesh in FreeFem++. Here we consider the function `buildlayers` in which a 3D domain is generated from a 2D one by making a sequence of horizontal layers. In our case, we take the 3D unit cube $[0,1]^3$ which is generated from the 2D unit cube $[0,1]^2$. The problem is

$$\left\{\begin{array}{lll} -\Delta u = f & \text{in} & \Omega_{3D} = [0,1]^2 \times [0,1] \\ \frac{\partial u}{\partial n} = \alpha(u_e - u) & \text{on} & \text{face number 2} \\ \frac{\partial u}{\partial n} = 0 & \text{on} & \text{the rest of the boundary,} \end{array}\right. \tag{7}$$

where now $u = u\,(x, y, z)$ and face number 2 is the face $\{x = 1\}$. In its weak or variational form, the problem reads as

$$\int_\Omega \nabla u \cdot \nabla v \; dxdydx + \int_{\text{face n}^o\ 2} \alpha uv \; d\Gamma - \int_{\text{face n}^o\ 2} \alpha u_e v \; d\Gamma - \int_\Omega fv \; dxdydz = 0 \quad \forall v.$$

Note that now $v = v\,(x, y, z)$ does not vanish on the boundary.

```
// Poisson’s equation on the 3D unit cube
load ’’msh3’’ // we need msh3 in 3D
mesh Th2=square(10,10);//2D mesh
int ncapas=10; // number of horizontal layers on the z-axis
real zmin=0, zmax=1;
mesh3 Th=buildlayers(Th2,ncapas,zbound=[zmin,zmax]); //3D mesh
real alpha=0.25, ue=25;
func 1000.*(x>0.4)*(x<0.6)*(y>0.4)*(y<0.6)*(z>0.4)*(z<0.6);
fespace Vh(Th,P13d); //P1 Lagrange finite elements in 3D
Vh u,v; // u,v belong to Vh
// and now we use macros to simplify expressions
macro grad(u) [dx(u),dy(u),dz(u)] //EOM

solve lapace3d(u,v)=int3d(Th)(grad(u)’*grad(v))
                   +int2d(Th,2)(alpha*u*v)
                   -int3d(Th)(f*v)
                   -int2d(Th,2)(alpha*ue*v);
plot(u);
```

A possible physical interpretation of this problem is the following: A body that occupies the region Ω has an internal heat source f. All the faces of the cube Ω are isolated except the face $x = 1$ where there is a convective heat flux modelled by Newton's law of cooling: heat transfer ($\kappa\frac{\partial u}{\partial n}$) takes place at a rate proportional ($-\alpha$) to the difference of temperature between the solid (u) and the surrounding (u_e). The thermal conductivity of the material, κ, has been normalized to 1. $u(x, y, z)$ represents the temperature at the point (x, y, z) at the stationary state. Figure 3 displays a cut plane picture of the solution. It is observed that temperature is higher on the internal region where heat is generated an decreases as we approach the face $x = 1$ where there exists a heat transfer to the surrounding.

3.3 Transient heat equation

FreeFem++ has two building blocks: the elliptic PDE system solver problem `solve`, and the convection module `convect`. However, there is also the possibility of implementing our own algorithms like the following example shows. Precisely, we shall solve the following evolution problem for the heat equation:

$$\left\{\begin{array}{lll} \frac{\partial u}{\partial t} - \nabla\cdot(\kappa\nabla u) = 0 & \text{in} & \Omega\times(0,T) \\ u\,(x,y,0) = u_0(x,y) & \text{in} & \Omega \\ \kappa\frac{\partial u}{\partial n} + \alpha\,(u-u_e) = 0 & \text{on} & \partial\Omega\times(0,T)\,. \end{array}\right. \tag{8}$$

Here $u = u\,(x, y, t)$ stands for the temperature at position (x, y) and time t, and $u_0(x, y)$ is the initial temperature. For simplicity, we take $\Omega = (0, 6) \times (0, 1)$. The thermal conductivity is given by

$$\kappa\,(x,y) = \left\{\begin{array}{lll} 1 & \text{if} & y < 0.5 \\ 0.2 & \text{else.} & \end{array}\right.$$

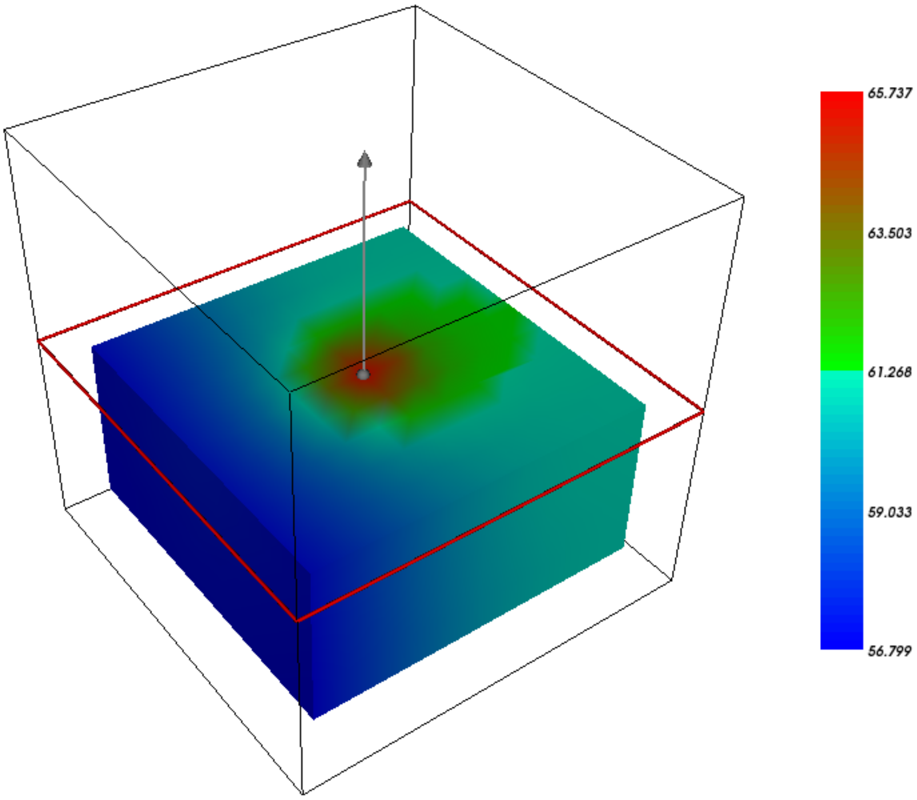

Figure 3: Picture of the solution of problem (7) obtained with the above code.

As in the preceding example, the boundary condition reflects Newton's law of cooling. To obtain the variational formulation of (8) we proceed as in the stationary case. To begin with, we multiply the PDE by some test function $v = v(x, y)$. Then, we integrate over Ω and apply integration by parts formula. We get

$$\int_{\Omega} \frac{\partial u}{\partial t} v \; dxdy - \int_{\partial\Omega} \kappa \frac{\partial u}{\partial n} v \; d\Gamma + \int_{\Omega} \kappa \nabla u \cdot \nabla v \; dxdy = 0.$$

Finally, we impose the boundary condition to obtain

$$\int_{\Omega} \frac{\partial u}{\partial t} v \; dxdy + \int_{\partial\Omega} \alpha (u - u_e) \, v \; d\Gamma + \int_{\Omega} \kappa \nabla u \cdot \nabla v \; dxdy = 0 \quad \forall v. \tag{9}$$

Next, we discretize the time variable by using an implicit Euler scheme. For the convergence properties of this scheme we refer the reader to [6]. Let us denote by $dt = T/N$, with $N \in \mathbb{N}$ fixed , and by $u_n = u(t_n)$, with $t_n = ndt$, $0 \le n \le N$. Then, we have

$$\frac{\partial u}{\partial t} \approx \frac{u_n - u_{n-1}}{dt}.$$

Substituting this expression into (9),

$$\int_{\Omega} \frac{u_n - u_{n-1}}{dt} v \; dxdy + \int_{\partial\Omega} \alpha (u_n - u_e) \, v \; d\Gamma + \int_{\Omega} \kappa \nabla u_n \cdot \nabla v \; dxdy = 0 \quad \forall v,$$

which is the discrete weak formulation that we implement in FreeFem++ next.

```
// transient heat equation
func u0=10+90*x/6; //initial temperature
func k=1.8*(y<0.5)+0.2; // thermal conductivity
real ue=25; //outside temperature
real alpha=0.25;
real T=0.7; //final time
real dt=0.1; //time step
mesh Th=square(30,5,[6*x,y]); // domain
fespace Vh(Th,P1); // Lagrange P1 finite elements
Vh u=u0,v,uold;
Vh[int] sol((T/dt)+1);
// variational formulation. Implicit Euler scheme
problem calor(u,v)=int2d(Th)(u*v/dt+k*(dx(u)*dx(v)+dy(u)*dy(v)))
                   +int1d(Th,1,2,3,4)(alpha*u*v)
                   -int1d(Th,1,2,3,4)(alpha*ue*v)
                   -int2d(Th)(uold*v/dt);
ofstream ff(''calor.dat''); // to generate a data file
for(int j=0;j<T/(dt);j=j+1)
{
 uold=u;
 calor;
 sol[j+1]=u; // to store the solution at different times
 ff<<u(3,0.5)<<endl;// calor.dat saves temperature at the point (3,0.5)
 }
plot(sol[0],value=true,ShowAxes=0,ColorScheme = 1,ps="sol_t0.eps");
plot(sol[5],value=true,ShowAxes=0,ColorScheme = 1,ps="sol_t05.eps");
plot(sol[10],value=true,ShowAxes=0,ColorScheme = 1,ps="sol_t1.eps");
plot(sol[20],value=true,ShowAxes=0,ColorScheme = 1,ps="sol_t2.eps");
```

Figure 4 shows the iso-thermal lines of the solution of problem (8) at some discrete times. These pictures simulate how air cools a rectangular plate which has an initial temperature $u_0(x, y)$ and a discontinuous thermal conductivity coefficient. Notice that at time $t = 0$, the temperature at the right-hand edge is 100 and the temperature at left-hand edge is 10. Then, as time evolves there is a heat flux from the heat region to the cold one.

3.4 Lamé system in 2D

In this example we move on a system of PDE, precisely, the Lamé system of linear elasticity in the plane. Consider a plate as shown in Figure 5 (top). Assume that the left vertical side of the plate is fixed and that there is no boundary force on the lower, upper, right sides and on the boundary of the interior circle. The body force is given by $\mathbf{f} = (0, -1)$. When the displacement $\mathbf{u} = (u_1, u_2)$ is small

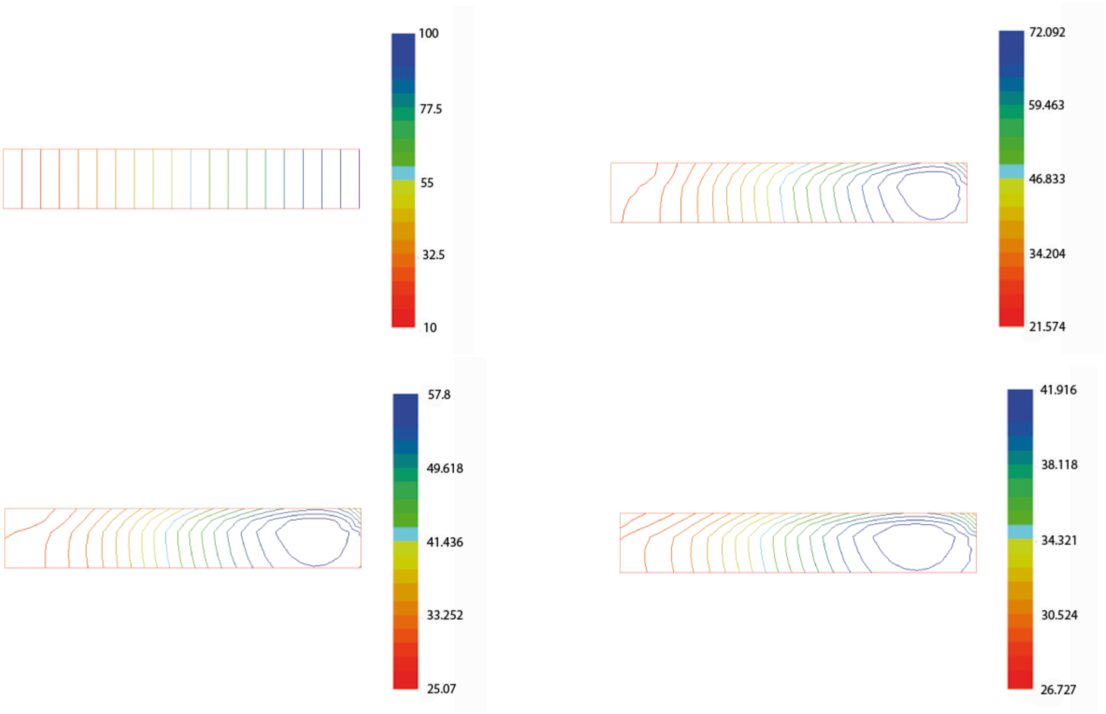

Figure 4: From left to right and from top to bottom, pictures of the FEM solution of problem (8) at times $t = 0$ (top left), $t = 0.5$, $t = 1$ and $t = 2$ (bottom right).

and the material is (linear) elastic, in the stationary case the following conditions are satisfied

$$\begin{cases} -\nabla\cdot\sigma = \mathbf{f} & \text{in} \quad \Omega \\ \mathbf{u} = 0 & \text{on} \quad \text{left side} \\ \sigma\cdot\mathbf{n} = \mathbf{0} & \text{on} \quad \text{the rest of the boundary,} \end{cases} \tag{10}$$

with

$$\sigma_{ij}\left(\mathbf{u}\right) = \lambda\delta_{ij}\text{trace}\left(\varepsilon\right) + 2\mu\varepsilon_{i,j}, \quad 1 \leq i, j \leq 2,$$

the stress tensor, where $\delta_{ij} = 1$ if $i = j$, 0 otherwise, λ, μ are the Lamé coefficients which describe the mechanical properties of the material, and

$$\varepsilon_{ij}\left(\mathbf{u}\right) = \frac{1}{2}\left(\frac{\partial u_i}{\partial x_j} + \frac{\partial u_j}{\partial x_i}\right), \quad 1 \leq i, j \leq 2$$

is the linearized strain tensor. As usual $\mathbf{n}$ is the outward unit normal vector. The variational form of (10) is

$$\int_\Omega \sigma\left(\mathbf{u}\right) : \varepsilon\left(\mathbf{v}\right)\ dxdy - \int_\Omega \mathbf{f}\cdot\mathbf{v}\, dxdy = 0 \quad \forall\mathbf{v} \text{ such that } \mathbf{v} = \mathbf{0} \text{ on left side.}$$

The notation $\sigma\left(\mathbf{u}\right) : \varepsilon\left(\mathbf{v}\right) = \sum_{i,j}\sigma_{ij}\varepsilon_{ij}$ stands for the contraction of σ and ε.

```
// Linear elasticity in 2D

//Domain and mesh
border a1(t=0,20){x=t;y=-1;label=1;};    //Lower side
border a2(t=-1, 1){x=20;y=t;label=2;};   //Right side
border a3(t=0,20){x=20-t;y=1;label=3;};  //Upper side
border a4(t=-1,1){x=0;y=-t;label=4;};   //Left side
border C(t=0, 2*pi){x=10+0.5*cos(t); y=0.5*sin(t);}; //Interior circle
//We define the meh from a1,a2,a3,a4 and C
mesh Th=buildmesh(a1(100)+a2(10)+a3(100)+a4(10)+C(-10));
plot(Th,wait=true); //Plots the mesh

fespace Vh(Th,P2); //Finite elements (P2) space definition
Vh u,v,uu,vv;      //Variables difinition

//Some constants and physical parameters
real sqrt2=sqrt(2.);
real E = 21e5, nu = 0.28; //E: Young’s modulus, nu: Poisson’s ratio
real lambda = E*nu/((1+nu)*(1-2*nu)), mu= E/(2*(1+nu)); //Lame coefficients
real f = -1; //Body force

//We can define macros to make programming easier
macro epsilon(u,v)  [dx(u),dy(v),(dy(u)+dx(v))/sqrt2] // EOM
macro div(u,v) (dx(u)+dy(v)) // EOM

//Solving the problem in variational form
solve lame([u,v],[uu,vv])= int2d(Th)(
        lambda*div(u,v)*div(uu,vv)
        +2.*mu*( epsilon(u,v)’*epsilon(uu,vv) ) )
        - int2d(Th)(f*vv)
        + on(4,u=0,v=0);


//Ploting the result
real coef=100; //A coefficient of amplification
mesh Thd = movemesh(Th, [x+u*coef, y+v*coef]);
plot(Thd,wait=1); //Result as a deformed mesh
real dxmin  = u[].min; //Minimum of displacement in x direction
real dymin  = v[].min; //Minimum of displacement in y direction
```

Sometimes it is interesting to obtain magnitudes that are not the solution of our PDE but can be evaluated from this solution. In the case of linear elasticity, it might be interesting to obtain, for example, the value of the von Mises stress. The von Mises stress is frequently used in engineering as a scalar representation of a 3–dimensional load state. This way, the yielding under any condition can be predicted from the results of simple uniaxial tensile tests.

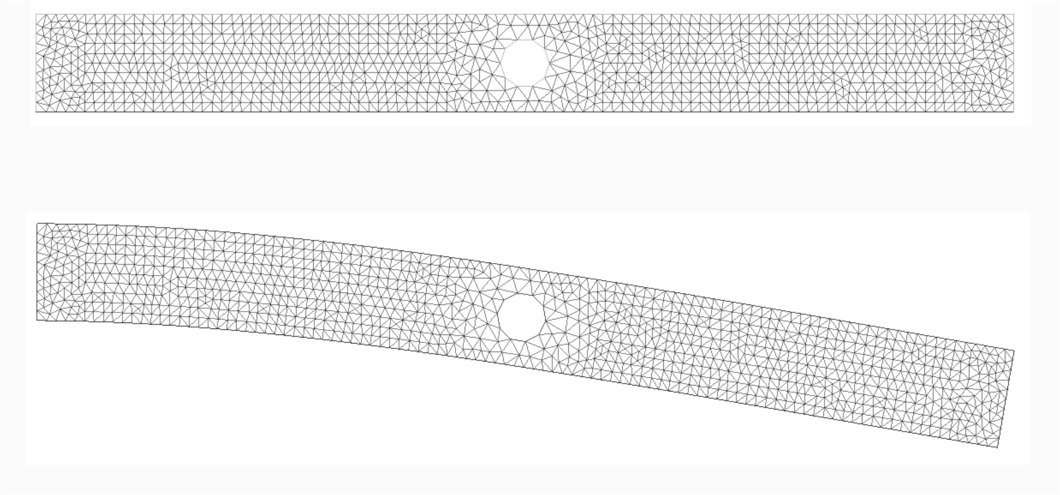

Figure 5: Initial mesh (top) and solution as a deformed mesh (bottom).

For a 2D problem the von Mises stress is

$$\sigma_{vm} = \sqrt{\sigma_{11}^2 - \sigma_{11}\sigma_{22} + \sigma_{22}^2 + 3\sigma_{12}^2}. \tag{11}$$

The next piece of code shows how to obtain and plot this value. The result is plotted in Figure 6.

```
//Obtaining the von Mises stress
fespace Wh(Th,P1); //We can define a new finite elements space
Wh Sigmavm;

//Stress tensor (since it is symmetric, it is enough with 3 elements)
macro Sigma(u,v) [2*mu*dx(u)+lambda*(dx(u)+dy(v)),
                  2*mu*dy(v)+lambda*(dx(u)+dy(v)),mu*(dy(u)+dx(v))]//EOM

//Von Mises stress
Sigmavm = sqrt(Sigma(u,v)[0]*Sigma(u,v)[0]-Sigma(u,v)[0]*Sigma(u,v)[1]
               +Sigma(u,v)[1]*Sigma(u,v)[1]+3*Sigma(u,v)[2]*Sigma(u,v)[2]);
plot(Sigmavm); //Ploting the result

real Sigmavmmax = Sigmavm[].max; //Max. von Mises stress
cout << " Max von Mises Stress  = " << Sigmavmmax << endl;
```

3.5 Skin effect in AC power electromagnetics

Next example shows the skin effect when AC current is carried by a wire of copper with circular cross section. The propagation of plane electromagnetics waves may be modeled by a complex Helmholtz's

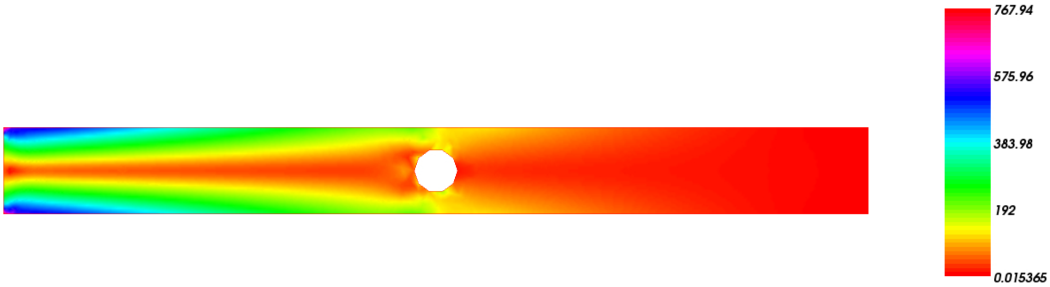

Figure 6: Von Mises stress. We can see that the maximum stress concentrates on the lower left corner.

equation for the electric field, namely,

$$\begin{cases} -\nabla\cdot\left(\frac{1}{\mu}\nabla E_c\right)+(i\omega\sigma-\omega^2\varepsilon)E_c=0 & \text{in} \quad \Omega=\{(x,y)\in\mathbb{R}^2 : x^2+y^2<0.1\} \\ E_c=1/\sigma & \text{on} \quad \partial\Omega, \end{cases} \tag{12}$$

where $E_c = E_c\,(x, y)$ is the complex electric field, σ is the conductivity, μ is magnetic permeability, ε is the coefficient of dielectricity, ω is angular frequency, and i stands for the pure imaginary number (also denoted by j in Electricity). The boundary condition indicates that, due to induction, the current density in the interior of the conductor is smaller than at the outer surface where it is set to 1.

A weak solution of (12) is a complex function $E_c = u + 1/\sigma$, with $u \in H_0^1\,(\Omega;\mathbb{C})$, such that u satisfies

$$\int_\Omega \frac{1}{\mu}\nabla u\cdot\nabla v\;dxdy+\int_\Omega(i\omega\sigma-\omega^2\varepsilon)u\cdot v\;dxdy=\int_\Omega -(i\omega\sigma-\omega^2\varepsilon)1/\sigma v\;dxdy \quad \forall v\in H_0^1\,(\Omega;\mathbb{C})\,.$$

The FreeFem++ code for this problem is the following.

```
// physical parameters
real sigma=57*1e+6;
real mu=4*pi*1e-7;
real omega=2*pi*50;
//real omega=2*pi*1; a lower value for angular frequency
real epsilon=8.8*1e-12;
// domain and mesh
border C(t=0,2*pi){x=0.1*cos(t);y=0.1*sin(t);};
mesh Th=buildmesh(C(50));
// space of complex finite elements P1
fespace Vh(Th,P1);
Vh<complex> u,v;
// solving the variational formulation
solve electro(u,v)=int2d(Th)((1/mu)*(dx(u)*dx(v)+dy(u)*dy(v))
                       +(omega*sigma*1i-omega*omega*epsilon)*u*v)
                       +on(C,u=1/sigma);
plot(u,value=true,fill=true,ShowAxes=0,ColorScheme = 1,ps="fig_electro.eps");
```

Figure 7 displays the solution obtained with this code. It is observed that the largest values of the electric field are concentrated on the boundary. This is the so-called skin effect. We suggest the reader to play with different values of ω in the code to show how decreasing the frequency of the alternating current results in a decreasing of the skin effect.

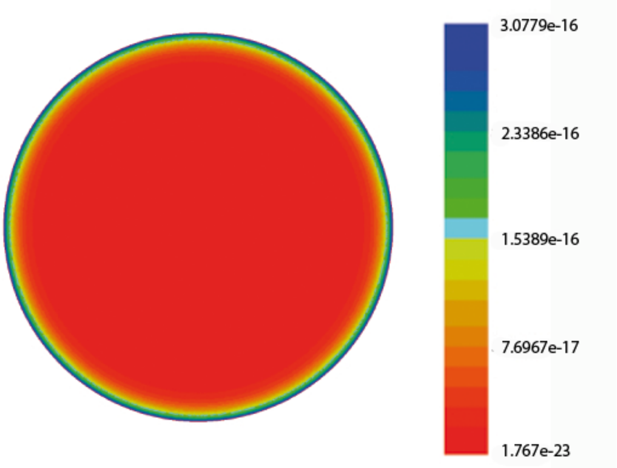

Figure 7: Picture of the modulus of E_c, solution of problem (12). It is observed that the largest values of this solution are concentrated on the boundary. This is the so-called skin effect.

3.6 Reynolds' equation in hydrodynamic lubrication

Consider the problem of lubricating the friction between a fixed rigid body presenting some abrupt edges, and a regular surface in movement by using an incompressible fluid in the separating region. This type of problems appears in real applications such as in feed-box or shaft-bearing systems. This problem may be modeled by the following Reynolds equation in lubrication theory (see [7])

$$\begin{cases} \left(\frac{U_0 h}{2} - \frac{h^3}{12\mu} p_x\right)_x + \left(\frac{V_0 h}{2} - \frac{h^3}{12\mu} p_y\right)_y = 0 & \text{in} \quad \Omega \\ p = p_0 & \text{on} \quad \partial\Omega, \end{cases} \tag{13}$$

where $\Omega = [0,1]^2$, $p = p(x,y)$ is the fluid pressure, μ is the fluid viscosity, $h = h(x,y)$ represents the distance between the surface and the solid, and (U_0, V_0) is the velocity of the surface.

A weak solution of (13) is a function $p = u + p_0$, with $u \in H_0^1(\Omega)$ such that

$$\int_\Omega \frac{h^3}{12\mu} \nabla u \cdot \nabla v \, dxdy = \int_\Omega \frac{h}{2} (U_0, V_0) \cdot \nabla v \, dxdy \quad \forall v \in H_0^1(\Omega).$$

We take a discontinuous h to model an abrupt edge on the body, e.g.,

$$h(x,y) = \begin{cases} 0.2, & 0 \le x \le 0.5 \\ 0.8, & 0.5 < x \le 1. \end{cases}$$

Since in the left-side term of the PDE we compute the partial derivative of h with respect to x, we get a Dirac mass type right-hand side term for the equation. This implies that the solution is not differentiable at $x = 0.5$. Consequently, in order to properly capture this singularity is very convenient to refine the mesh in this region. We use the FreeFem++ function `adaptmesh` for this purpose.

```
real mu=0.391; // viscosity
mesh Th=square(100,100); // surface
plot(Th);
func h=0.2+0.6*(x>0.5); // separation between surface and solid
real U0=10, V0=5; // surface velocity
fespace Vh(Th,P1); // P1 elements
Vh p,v; // p=pressure
// variational formulation
problem lubrica(p,v)=int2d(Th)(((h^3)/(12*mu))*(dx(p)*dx(v)+dy(p)*dy(v)))
                     -int2d(Th)((h/2)*(U0*dx(v)+V0*dy(v)))
                     +on(1,2,3,4,p=1);
lubrica;
plot(p);
Th=adaptmesh(Th,p); // refine mesh according to singularities of p
lubrica;
plot(Th,p,value=true,fill=true,ColorScheme = 1,ps="fig_lubrica.eps");
```

Figure 8 shows the pictures of both the refined mesh and the solution of problem (13). It is observed that the largest values of p are located at the same place where there is the discontinuity of the function h, i.e. $x = 0.5$, which models the separation between the surface and the solid. Also, Figure 8 seems to indicated that p is not differentiable at $x = 0.5$ in agreement with the theoretical results in [7].

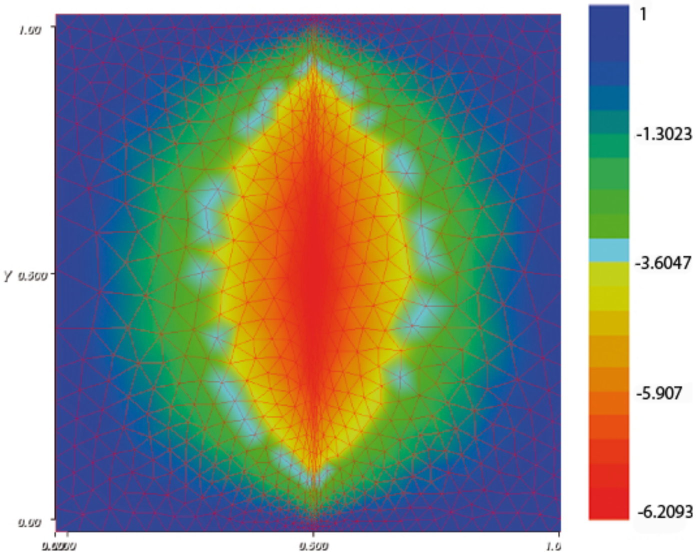

Figure 8: Picture of pressure $p(x, y)$, solution of (13).

Acknowledgements. The authors express their gratitude to the FreeFem++ team in Paris IV for providing us with this wonderful free software. Also, the second author is very grateful to Professor

Miguel Sanz Alix (University of Valencia) who introduced him variational methods for PDE, and to José Antonio Vallejo for his kind invitation to the Fourth Summer School UVEG-UASLP held at Universidad Autónoma of San Luís Potosí (Mexico) where a part of this paper was written. This work was partially supported by project 08720/PI/08 from Fundación Séneca (Agencia de Ciencia y Tecnología de la Región de Murcia, Spain, II PCTRM 2007-10).

References

[1] Babuška, I., Error-bounds for finite element method. Numer. Math. (1970/1971) 16, 322-333.

[2] Evans, L. C., Partial Differential Equations, 1998 (Graduate Studies in Mathematics 19 American Mathematical Society).

[3] F. Hecht, A. Le Hyaric, O. Pironneau, K. Ohtsuka, Tutorial FreeFem++ . Available at http://www.freefem.org/

[4] Periago, F., A first step towards variational methods in engineering, Int. J. Math. Educ. Sci. Technol. (2003) 34, no. 4, 549-559

[5] Periago, F., Modelización matemática y simulación numérica en Ingeniería, Notes of a Master Course (in Spanish). Available at the web site http://filemon.upct.es/˜fperiago/

[6] Raviart, P. A., Thomas, J. M., Introduction à l'Analyse Numérique des Équations aux Dérivées Partielles, 1988 (Masson).

[7] Tello, J. I., Regularity of solutions to a lubrication problem with discontinuous separation data. Nonlinear Anal. 53 (2003), no. 7-8, 1167-1177.

[8] Xia, X., Computing multiple integrals by MatLab, The Electronic Journal of Mathematics and Technology, (2012) 6, n 2, 159-174.